九州大学学術情報リポジトリ
Kyushu University Institutional Repository

A Study on the Correlation of Structure and Fluidity of Three Asian Coal Ashes and Slags

Lin, Xiongchao
Interdisciplinary Graduate School of Engineering Sciences, Kyushu University

Ideta, Keiko
Institute for Materials Chemistry and Engineering, Kyushu University

Miyawaki, Jin
Institute for Materials Chemistry and Engineering, Kyushu University

Takebe, Hiromichi
Graduate School of Science and Engineering, Ehime University

他

https://hdl.handle.net/2324/21036

出版情報：Journal of Novel Carbon Resource Sciences. 5, pp.5-9, 2012-02. Kyushu University G-COE program "Novel Carbon Resource Sciences" secretariat
バージョン：
権利関係：

Kyushu University Global COE Program
Journal of Novel Carbon Resource Sciences, Vol. 5, pp. 5-9, Feb. 2012

A Study on the Correlation of Structure and Fluidity of Three Asian Coal Ashes and Slags

Xiongchao Lin[*1], Keiko Ideta[*2], Jin Miyawaki[*2], Hiromichi Takebe[*3], Seong-Ho Yoon[*2], Isao Mochida[*2]

[*1]Interdisciplinary Graduate School of Engineering Sciences, Kyushu University
[*2]Institute for Materials Chemistry and Engineering, Kyushu University
[*3]Graduate School of Science and Engineering, Ehime University

(Received November 2, 2011; accepted December 5, 2011)

Correlations among structures and flow properties of three typical Asian coal ashes and their slags were carefully examined using multi-nuclear solid-state NMR and self-manufactured viscometer. The amorphous structures of slags were successfully quantified through the NMR measurement. The Si structure of slag D which showed highest viscosity among three slags was mainly Q^4 structures with a high degree of polymerization. Slag M which contained high Fe content showed similar Si structure to that of slag D. Alkaline-earth ions of Ca^{2+} and Mg^{2+} in slag A successfully segmented the framework to form the primary Q^2 structures, which resulted in the lowest viscosity of slag A.

1. Introduction

Coal ash is a complex material, and detailed knowledge is required to comprehensively understand and predict key physical properties of its melt to enable continuous operation of gasification. In particular, the melt must have an appropriate viscosity at the combustion temperature for commercial gasification[1-5].

The optimum viscosity at the critical temperature is necessary to achieve successful slag tapping. Consequently, various concepts and models have been proposed to estimate molten viscosity according to the ash composition. Previous studies mainly relied on simulations and the phase diagram to identify the roles and effects of individual components[6,7]. But each of them has limitations and drawbacks. The exact function of every component, especially in the molten state, needs to be clarified.

In this study, we aimed at clarifying the correlations between the structure and melt viscosity of coal ashes and slags. For carrying out the study, we chose three typical Asian coal ashes. They possessed high SiO_2 and Al_2O_3, high iron oxide, and medium CaO and iron oxide contents, respectively. Their slags were obtained through rapid quenching after the gasification in the gasification pilot plant under the optimum conditions. Low-temperature ashes (LTA) were prepared at low temperature of 300°C in the laboratory. They were analyzed with X-ray fluorescence spectroscopy (XRF), X-ray diffraction measurement (XRD) and 800 MHz (for ^1H) multi-nuclear solid-state nuclear magnetic resonance (SS-NMR) at a magnetic field of 18.8 T. Melt viscosities were also measured up to 1700°C using a high-temperature rotary viscometer. Flow properties and their microstructures were used to develop viscosity-structure correlations for the slags.

2. Experimental

2.1 Samples

Some properties of coals (Datong coal from China and Malinau and Adaro coals from Indonesia) and their ashes ((Datong coal ash denoted as ash D, and Malinau and Adaro coal ashes denoted as ash M and ash A, respectively) are summarized in Table 1. LTAs were prepared by heating at 300°C in air for 60-day to remove the organic components to attain the minimized changes of inherent structures of minerals in the original coals. Rapidly-quenched slags which were produced in the oxygen-blown type gasifier were supplied from the Japanese company (J-Power Co. Ltd.).

2.2 Viscosity measurement

Viscosity was measured under a nitrogen atmosphere up to 1700°C using a self-manufactured high-temperature rotary type viscometer equipped with a high-purity alumina rotor and crucible. The diameter of the alumina rotor and the internal diameter of the alumina crucible were 6.00 ± 0.02 mm and 37.60 ± 0.05 mm, respectively. The viscometer was calibrated using the reference material 717a (borosilicate glass, certificated by the American National Institute of Standards & Technology). The deviation was carefully controlled to less than 5 %.

2.3 Analyses

The chemical compositions of the samples were determined by XRF (SHIMADZU-EDX800). XRD was carried out using Cu Ka radiation at 40 kV and 30 mA at room temperature using a Rigaku RINT Ultimate-III powder diffractometer equipped with a graphite monochromator and NaI (TI) detector. The XRD scans were performed between 5 and 90°, with a step of 0.02°/s.

An 800 MHz multi-nuclear SS-NMR (JEOL-ECA800) instrument was used to characterize the aluminum and

Table 1 Properties of coal samples used in this study.

Samples	D	M	A
Proximate Analyses (%)			
Moisture	4.18	4.41	9.91
Ash	11.40	2.81	2.49
Volatiles	24.52	34.39	43.10
Fixed carbon	59.90	58.39	44.50
Ultimate Analyses (%) [a]			
Carbon	75.26	77.35	72.85
Hydrogen	5.57	5.73	4.91
Nitrogen	1.39	1.42	0.98
Oxygen(*diff.*)	17.66	15.39	21.15
Sulfur	0.12	0.10	0.10
Elemental compositions of ashes (wt %) [b]			
SiO_2	55.56	29.57	33.30
Al_2O_3	28.12	19.69	17.6
Fe_2O_3	11.52	32.16	16.56
CaO	1.38	7.23	16.8
K_2O	1.18	1.23	1.10
TiO_2	0.97	1.47	1.26
SO_3	0.57	5.35	6.27
P_2O_5	0.36	ND[c]	ND[c]
MgO	ND[c]	2.68	6.64
ZrO_2	ND[c]	0.03	0.01
Total	99.60	99.41	99.54
B/A[d]	0.19	0.85	0.90

[a] Analyses under dry mineral matter free basis
[b] Ashes were prepared according to JIS M8815. Trace elements (*e.g.*, Sr, Mn, V, Y, Zn, Cu, Rb) were ignored.
[c] Not detected.
[d] $B=\%Fe_2O_3+\%CaO+\%MgO+\%Na_2O+\%K_2O$; $A=\%SiO_2+\%Al_2O_3+\%TiO_2$

silicon nuclei in powdered samples. High-resolution ^{29}Si-NMR spectra were obtained at a frequency of 158.96 MHz under the single-pulse mode up to 20 kHz using 3.2 mm zirconia rotors. The spectra were obtained with π/10 pulses of 9.2 ms, 20 s recycle time, and collected over 40000 free induction decay (FID) signals. ^{27}Al NMR spectra were acquired at a spinning rate of 20 kHz by applying an 18.8 T (Larmor frequency for ^{27}Al of 208.48 MHz) narrow bore magnet. The chemical shift scale in ppm was referenced to aqueous 1.0 M $AlCl_3$.

3. Results and discussion

3.1 Characterization of coal and ashes

The results of coal analyses and elemental compositions of the ashes are listed in Table 1. Silica, alumina, iron oxide and calcium oxide comprised the principal components. The B/A ratios of the ashes were calculated according to the equation $B/A=(\%Fe_2O_3 + \%CaO + \%MgO + \%Na_2O + \%K_2O) / (\%SiO_2 + \%Al_2O_3 + \%TiO_2)$ [8]. Ash D, with high SiO_2 and Al_2O_3 contents, had a low B/A ratio of 0.19; ashes M and A had similar B/A values of 0.85 and 0.90, respectively.

3.2 XRD analysis

Figure 1 shows the XRD patterns of LTAs. All three LTAs comprised mainly kaolinite and quartz. The LTA D also showed peaks of rutile, siderite, and hematite. For LTA M with the high iron content, intense siderite peaks and a weak hematite peak were observed.

Figure 2 shows the XRD patterns of the slags. All of these XRD patterns showed broad peaks, indicating amorphous or vitreous character resulting from the rapid quenching of the molten ashes from the gasifier.

Based on knowledge of the ash components, we assigned the broad peak at 13-33° in slag D to amorphous alumina-silicate and silica, the broad peak at 15-35° in slag M to the amorphous iron-rich minerals and alumina-silicate, and the broad peak at 17-37° in ash A to amorphous (Ca, Mg)-bearing minerals derived from the destruction of the crystal structure as a result of rapid quenching. However, the XRD technique apparently has a limitation to obtain detailed structural information on slags.

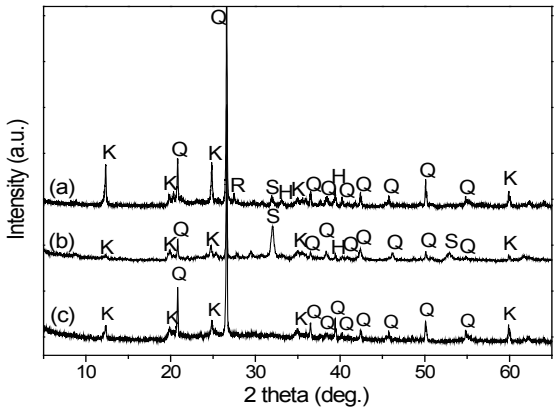

Fig. 1 XRD patterns of LTAs; (a) D, (b) M, and (c) A. Labeled peaks correspond to K: kaolinite-$Al_2(Si_2O_5)(OH)_4$ (PDF#06-0221); Q: quartz-SiO_2 (α-PDF#77-1060); R: rutile-TiO_2 (PDF#21-1276); H: hemitate-Fe_2O_3 (PDF#24-0072); and S: siderite-$FeCO_3$ (PDF#29-0696).

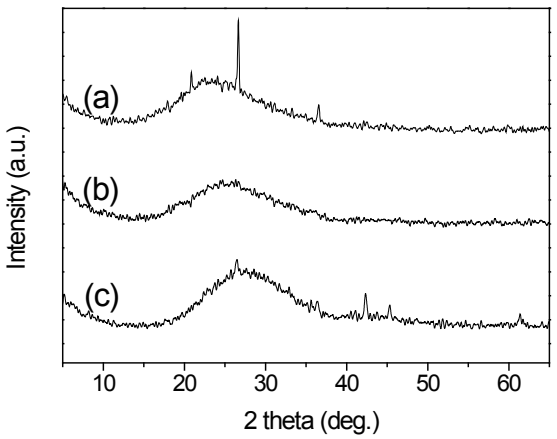

Fig. 2 XRD patterns of (a) D, (b) M, and (c) A slags obtained by rapid quenching of molten ashes from gasifier.

3.3 Solid-state NMR analysis

Although the slags were identified by XRD, the lack of contrast between minerals and also the associated alumina-silicate glass made it difficult to analyze the compositions separately. The amorphous structures of coal ash remain largely unexplored because of the difficulty associated with their quantitative evaluations. However, NMR spectroscopy provides a powerful way to quantify the local chemical and the structural environments, which can be effectively used to examine the structures of amorphous ash or slag.

3.3.1 Analysis of LTAs

Figure 3 shows the ^{29}Si and ^{27}Al SS-NMR spectra of the LTAs. In the ^{29}Si spectra (Figure 3(I)), main resonances were observed at -92.3 ppm of kaolinite and -107.5 ppm or -108.2 ppm of quartz. For Al, resonance in the region from 5.4 to 6.4 ppm was attributed to the 6-coordinated Al species of kaolinite. Besides, peaks at 72.2 ppm and 59.7 ppm were observed for LTA D, which was assigned to montmorillonite ($(Na,Ca)_{0.33}(Al,Mg)_2(Si_4O_{10})(OH)_2$). LTA M shows only two peaks at 5.4 ppm and 69.5 ppm, indicating that principal minerals in LTA M were kaolinite and muscovite ($KAl_2(AlSi_3O_{10})(OH)$). LTA A showed similar three peaks with LTA D ash.

The NMR analyses indicated that LTAs predominantly comprised of aluminosilicate minerals.

3.3.2 Analysis of slags

Figure 4 shows the ^{29}Si SS-NMR spectra of the slags. Deconvolution was carried out by assuming Gaussian profiles but, because the peaks were very broad, such deconvolution could not provide a fully exact structural distribution.

Q^n structural theory was applied to clarify the contributions of the different structures in the mixed minerals[9-14]. Tetrahedral SiO_4 units (TO_4 unit) were identified according to their mutual connectivity as $Q^n = [Si(OSi)_{n-m}(OAl)_m]_n(M)_{4-n}$, where n indicates the number of binding oxygens (BOs) within a SiO_4 tetrahedron, m is the number of neighboring tetrahedral AlO_4 units (TO_4 units) *via* BOs (n = 1-4; m<n), and M denotes cations (*e.g.*, Ca^{2+}, Mg^{2+}, *etc.*). Because extensive overlapping was observed, several standard materials (such as: quartz, Q^4, -107.3 ppm; anorthite, Q^4, -83.0 ppm; wollastonite, Q^2, -86 ppm; and diopside, Q^2, -85 ppm, *etc.*) were used to assign the deconvoluted spectra in Figure 4.

Slag D consists mainly go Q^4 due to the high silica and alumina contents; five components were identified at -110.2 ppm, -104.3 ppm, -99.5 ppm, -93.4 ppm, and -86.0 ppm (Figure 4 I (a)), attributed to Q^4(0Al), Q^4(1Al), Q^4(2Al), Q^3(0Al), and Q^3(1Al), respectively. The peak of rapidly-quenched slag M was slightly broader and shifted downfield (Figure 4 I (b)); the deconvoluted peaks were assigned in the same way as those in the slag D. The

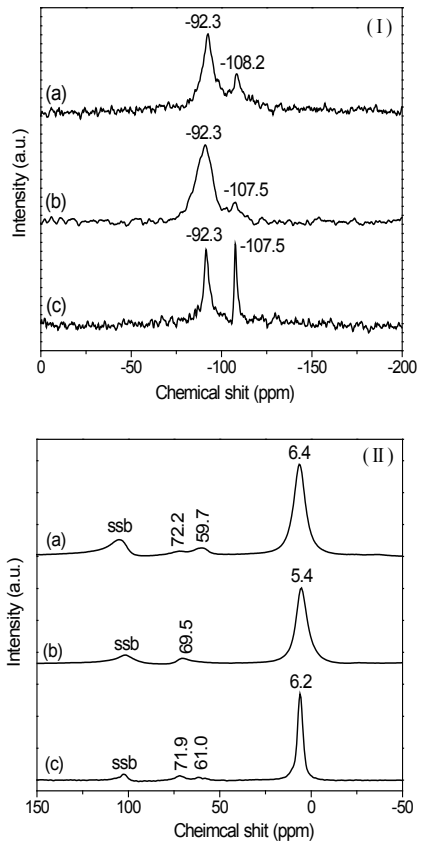

Fig. 3 (I) ^{29}Si and (II) ^{27}Al SS-NMR spectra of LTAs; (a) D, (b) M, and (c) A.

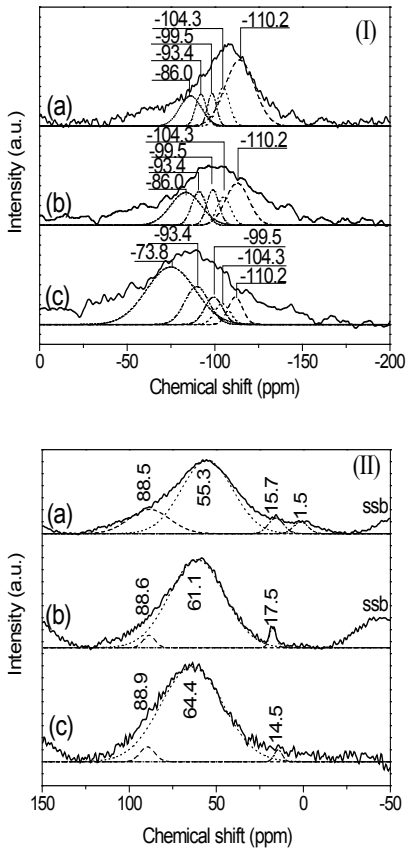

Fig. 4 (I) ^{29}Si and (II) ^{27}Al SS-NMR spectra of (a) D, (b) M, and (c) A slags obtained by rapid quenching of molten ashes from gasifier.

peak for slag A was apparently shifted downfield (Figure 4 I (c)). The peaks were deconvoluted to -110.2 ppm, -104.3 ppm, -99.5 ppm, -93.4 ppm, and -73.8 ppm, and were ascribed to Q^4(0Al), Q^4(1Al), Q^4(2Al), Q^3(0Al), and Q^2(1Al), respectively.

All the slags displayed resonances primarily due to four-coordinate aluminum. As shown in Figure 4 II (a), slag D showed four resonances. The peak at 1.5 ppm was assigned to poorly-crystalline mullite based on comparison to a reference sample. Another peak at 15.7 ppm was attributed to six-coordinate aluminum in α-alumina. The dominating four-coordinate structure appeared at 55.3 ppm. This resonance is due to tetrahedral aluminum comprising the T-O-T structure in slags. Slag M also showed two kinds of coordinate aluminum species (Figure 4 II (b)). The resonance at 17.5 ppm was ascribed to six-coordinate aluminum in α-alumina. Four-coordinate aluminum is the primary structure causing the signal at 61.1 ppm and was accompanied by a shoulder at 88.6 ppm. Resonances at 64.4 ppm and 88.9 ppm for slag A were ascribed to tetrahedral AlO_4 (Figure 4 II (c)). A weak peak at 14.5 ppm indicated low α-alumina content. It is interesting to note that the aluminum site distribution is not influenced significantly by the composition. The α-alumina found in the slags was likely from the cracks of the gasifier refractory[16].

Resonance intensity is plotted as a function of chemical shift in Figure 5. Slag D (Figure 5 (a)) had more components at higher chemical shifts, revealing the highest concentration of Q^4. That is, slag D principally consisted of silica, which formed the large framework. Slag M with significantly high iron content showed similar Q^4 and Q^3 amounts (Figure 5 (b)), indicating that the molten structure was composed principally of silica and aluminosilicate. In contrast, the rapidly-quenched slag A showed low Q^4 and Q^3 amounts, but remarkably high Q^2 amount (Figure 5 (c)), indicating depolymerization through the cutting of the framework by cations such as Ca^{2+} and Mg^{2+}.

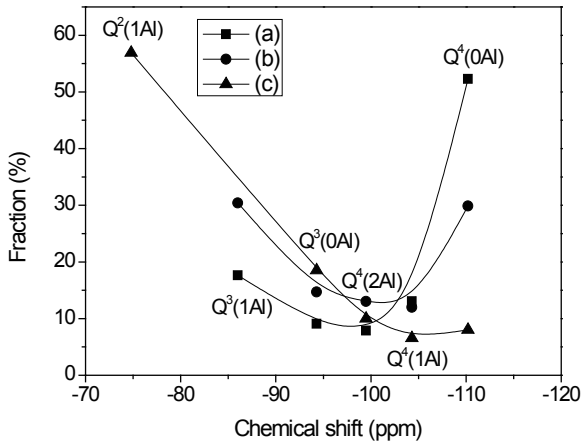

Fig. 5 Chemical shift fractional distributions of (a) D, (b) M, and (c) A slags after rapid quenching of molten ashes from gasifier.

3.4 Flow properties of slags with various structures

The flow characteristics of the molten ashes indicated shear-thinning behavior[17-19] or "pseudo-plastic" behavior[20] according to the shapes of the rheograms.

The flow pattern of slag D is non-Newtonian even up to 1700°C because of the large T-O-T framework structure (*e.g.*, Si-O-Al and Si-O-Si with a high degree of polymerization (Q^4) and high concentration of solid particles (*i.e.*, alumina, mullite) (Figure 6a).

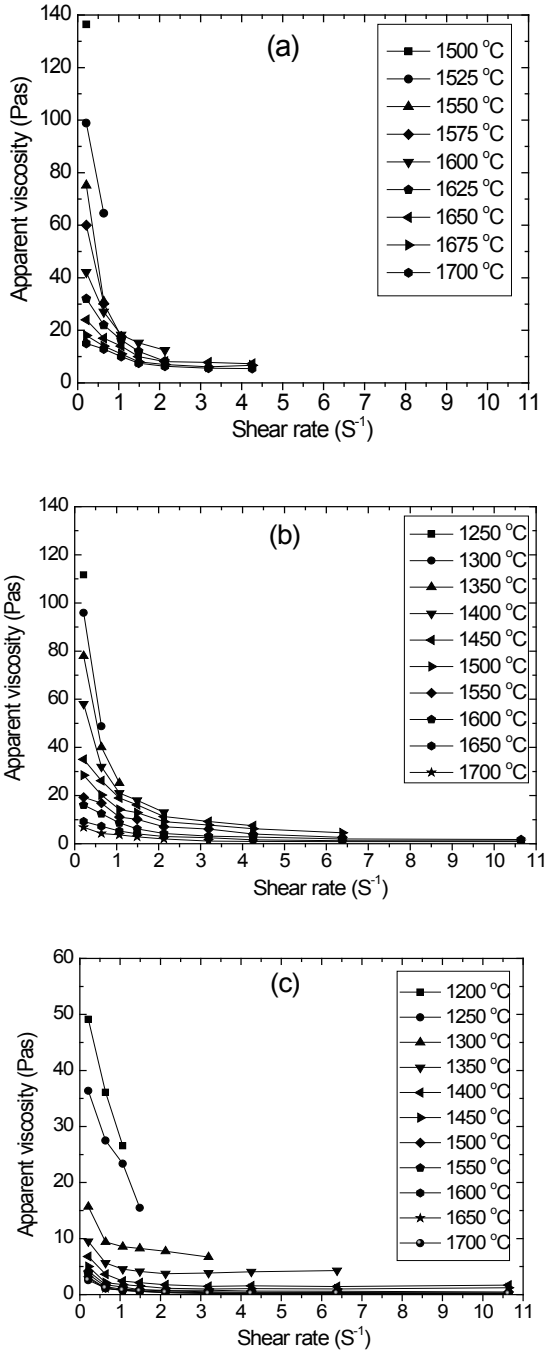

Fig. 6 Apparent viscosity as a function of shear rates of (a) D, (b) M, and (c) A slags after rapid quenching of molten ashes from gasifier.

Slag M approaches Newtonian flow above 1500°C, indicative of a liquid with few crystalline and/or solid particles (Figure 6b). Even though large numbers of T-O-T structures are still present, the polymeric structure is potentially easily broken down because the branches of the polymeric structure can be modified by iron (II) ions. Above 1500°C, laminar flow dominates, and below this temperature, the network exists as a blend of framework formers and modifiers. Solid particles and/or isolated crystals play a significant role in the shear-thinning behavior.

Short-segment microstructures with primary Q^2(1Al) in slag A demonstrated slight shear-thinning, even below the *Tcv* (Temperature of critical viscosity) (1250°C) (Figure 6c). The viscosity had Newtonian character above 1350°C, where suspended solid particles were minimal for this sample.

Consequently, the different structures of slags lead to the different viscosities, as shown in Figure 7. D slag with primary Q^4 structures has the highest viscosity; M slag containing high iron oxide shows lower viscosity; and A slag with main Q^2 structures demonstrates the lowest viscosity.

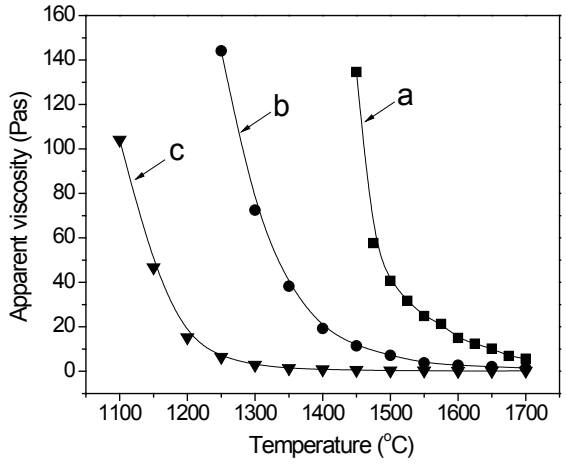

Fig. 7 Viscosity–temperature curves of (a) D, (b) M, and (c) A slags after rapid quenching of molten ashes from gasifier.

4. Conclusions

Correlations were developed among compositions, structures, and melt properties of three typical Asian coal ashes and their rapidly-quenched slags. The following conclusions were made: 1) The major structures in slags were Si and Al tetrahedral combining through T-O-T linkages; 2) Shifts in ^{29}Si resonances indicate that alkaline-earth ions segmented the framework and formed primarily Q^2 structures; 3) A large framework structure showed non-Newtonian flow and strong shear-thinning behavior. Segmental structures composed mainly of Q^2 structures maintained Newtonian flow until low temperatures and displayed less shear-thinning behavior.

Acknowledgements: The authors gratefully acknowledge the financial support provided by the New Energy Development Organization (NEDO) and the Global Center of Excellence (GCOE) of Kyushu University.

References

1) L. Q. Duan, R. M. Lin, S. M. Deng, H. G. Jin, R. X. Cai, *Energ. Convers. Manage.*, **45**, 797 (2004).
2) C. D. Sheng, Y. H. Lu, X. P. Gao, H. Yao, *Energ. Fuel*, **21**, 435 (2007).
3) S. Rezvani, Y. Huang, D. McIlveen-Wright, N. Hewitt, J. D. Mondol, *Fuel*, **88**, 2463 (2009).
4) J. C. Groen, D. D. Brooker, P. J. Welch, M. S. Oh, *Fuel Process Technol.*, **56**, 103 (1998).
5) G. W. Bryant, G. J. Browning, H. Emanuel, S. K. Gupta, R. P. Gupta, J. A. Lucas, T. F. Wall, *Energ. Fuel*, **14**, 316 (2000).
6) G. Urbain, F. Cambier, M. Deletter, M. R. Anseau, *Brit. Ceram. Trans. J.*, **80**, 139 (1981).
7) H. J. Hurst, F. Novak, J. H. Patterson, *Fuel*, **78**, 439 (1999).
8) H. H. Schobert, R. C. Streeter, E. K. Diehl, *Fuel*, **64**, 1611 (1985).
9) M. Templin, U. Wiesner, H. W. Spiess, *Adv. Mater.*, **9**, 814 (1997).
10) P. Pena, J. M. R. Mercury, A. H. de Aza, X. Turrillas, I. Sobrados, J. Sanz, *J. solid state chem.*, **181**, 1744 (2008).
11) J. Rocha, J. Klinowski, *Phys. Chem. Miner.*, **17**, 179 (1990).
12) R. K. Sato, P. F. Mcmillan, P. Dennison, R. Dupree, *Phys. Chem. Glasses*, **32**, 149 (1991).
13) M. Criado, A. Fernandez-Jimenez, A. Palomo, I. Sobrados, J. Sanz, *Micropor. Mesopor. Mat.*, **109**, 525 (2008).
14) C. A. Fyfe, K. C. Wongmoon, Y. Huang, H. Grondey, K. T. Mueller, *J. Phys. Chem.-U.S.*, **99**, 8707 (1995).
15) G. J. Kennedy, J. W. Wiench, M. Pruski, *Solid State Nucl. Mag.*, **33**, 76 (2008).
16) T. M. Besmann, *Calphad*, **32**, 466 (2008).
17) S. Wright, L. Zhang, S. Sun, S. Jahanshahi, *Metall Mater. Trans. B*, **31**, 97 (2000).
18) Y. L. Song, X. L. Liu, J. F. Chen, *Colloid Surface A*, **247**, 27 (2004).
19) W. J. Song, L. H. Tang, X. D. Zhu, Y. Q. Wu, Z. B. Zhu, S. Koyama, *Fuel*, **89**, 1709 (2010).
20) P. K. Senapati, B. K. Mishra, A. Parida, *Powder Technol.*, **197**, 1 (2010).